Soft tissue tumors: perfusion and diffusion-weighted MR imaging

Rijswijk, Catharina van

5

Chapter 5

Soft tissue tumors: value of static and dynamic Gd-DTPA-enhanced MR imaging in predicting malignancy

Catharina S.P. van Rijswijk, Maartje J.A. Geirnaerdt, Pancras C.W. Hogendoorn, Anthonie H.M. Taminiau, Frits van Coevorden, Aeilko H. Zwinderman, Thomas L. Pope, Johan L. Bloem

Radiology 2004; 233:493-502

ABSTRACT

PURPOSE:
To prospectively evaluate static and dynamic gadopentetate dimeglumine enhanced magnetic resonance (MR) imaging relative to nonenhanced MR imaging in differentiation of benign from malignant soft tissue lesions and to evaluate which MR parameters are most predictive of malignancy, with associated interobserver variability.
MATERIALS AND METHODS:
One-hundred-forty consecutive patients (78 male, median age 51 years and 62 female, median age 53 years) with a soft tissue mass underwent nonenhanced, static and dynamic contrast-enhanced MR imaging. Diagnosis was based on histologic findings in surgical specimens (86 of 140), findings of core-needle biopsies (43 of 140) or results of all imaging procedures with clinical follow-up (11 of 140). Multivariate logistic regression analysis was used to identify the best combination of MR parameters that might be predictive of malignancy. Subjective overall performance of two observers was evaluated using receiver operating characteristic analysis.
RESULTS:
For subjective overall diagnosis, the area under the receiver operating characteristic curve, a measure for the diagnostic accuracy, was significantly larger for the combined nonenhanced and contrast-enhanced MR imaging than it was for nonenhanced MR images alone, with no significant difference between both observers. Multivariate analysis of all lesions reveals that the combined interpretation of nonenhanced, static and dynamic contrast-enhanced MR parameters were significantly superior to nonenhanced MR parameters alone and nonenhanced parameters combined with static contrast-enhanced MR parameters in predicting malignancy. The most discriminating parameters are presence of liquefaction, start of dynamic enhancement (time interval between start of arterial and tumor enhancement) and lesion size. Results for extremity lesions were the same with one exception: with dynamic contrast-enhanced MR parameters diagnostic performance of one observer did not improve.
CONCLUSION:
Static and dynamic contrast-enhanced MR imaging, when added to nonenhanced MR imaging, improved differentiation between benign and malignant soft tissue lesions.

INTRODUCTION

Soft tissue sarcomas are rare lesions accounting for approximately 1% of all malignant tumors (1;2). The incidence of benign soft tissue tumors is much higher, although the exact incidence is unknown (3). Survival of patients with malignant soft tissue tumors depends mainly on adequate and timely resection and/or (neo)adjuvant chemotherapy (4;5), whereas benign tumors require less aggressive treatment. Imaging is used for not only local staging, but also differentiation between benign and malignant lesions and differentiation between viable tumor and components such as necrosis, hemorrhage, edema, cystic and myxoid degeneration, and fibrosis. This information is needed to decide on subsequent diagnostic and/or therapeutic action and to confirm or challenge results of other diagnostic procedures.

Magnetic resonance (MR) imaging with nonenhanced T1- and T2-weighted (fast) spin-echo sequences is a well-established imaging tool for the detection and local staging of soft tissue tumors (6-9). There is a wide range of specificity values of MR imaging in differentiation of benign from malignant soft tissue lesions reported in the literature (7;8;10-13). Berquist et al. and Moulton et al. found a relatively high specificity of 76-90% (11;14). Other researchers have reported that MR imaging has low specificity in differentiation between benign and malignant soft tissue masses with most lesions demonstrating a non-specific appearance (7;10;12;15). Patient selection may in part explain the differences in specificity of MR imaging.

The use of intravenously administrated gadopentate dimeglumine for characterizion of soft tissue tumors is controversial (16-22). However, there are no results of a prospective study with multivariate analysis reported in the literature. In addition, the interobserver variability of contrast-enhanced MR parameters has not been closely investigated. Only two large studies with static T1-weighted contrast-enhanced MR imaging have been published (18;20). May et al. (20) reviewed their experience with static contrast-enhanced MR imaging in 242 musculoskeletal lesions, which included 151 soft tissue lesions, and concluded that routine use of gadopentetate dimeglumine not justified. De Schepper et al. (18) retrospectively evaluated multivariate predictors of malignancy, which included static contrast-enhanced MR parameters, and confirmed the limited value of MR imaging in adequate characterization. Later, analysis of the pattern of contrast enhancement using dynamic MR data was proposed as a way of improving specificity (23-28). However, all reported dynamic contrast-enhanced MR studies have included musculoskeletal neoplasms that comprised a relatively small number of soft tissue lesions.

The conflicting and equivocal results on the usefulness of dynamic contrast-enhnaced MR imaging (16-28) in combination with the rapidly expending knowledge about angiogenesis in tumors prompted us to undertake this study prospectively. Our purpose was to prospectively evaluate static and dynamic contrast-enhanced magnetic resonance (MR) imaging relative to nonenhanced MR imaging in the differentiation of benign from malignant soft tissue lesions and to evaluate which MR parameters are most predictive of malignancy, with associated interobserver variability.

MATERIALS AND METHODS

Patients and Reference standard

Between March 1999 and February 2001, 140 consecutive patients (78 male, median age 51, range 7-79 years and 62 female, median age 53, range 1-85 years), with no significant difference in age distribution between sexes, underwent MR imaging at two tertiary referral hospitals for bone and soft tissue sarcomas. The indication for MR imaging in all patients was characterizion and local staging of a soft tissue mass with a clinical differential diagnosis that included soft tissue sarcoma. Patients with obvious clinically benign lesions, such as subcutaneous lipomas, were therefore excluded. Two additional patients were excluded because of motion artifacts; claustrophobia and problems with contrast agent administration were not encountered. Patients with lesions that originated from bone were not included.

In 140 patients, the standard of reference was based on histologic findings in surgical specimens in 86 (61%), findings of core-needle (MCN; US biopsy, Franklin, Ind) biopsies 43 (31%) or results of all the imaging procedures with inclusion of serial clinical follow-up for at least two years in 11 (8%). Lesions were classified according to the World Health Organization classification of Soft Tissue Tumors (2).

At both institutions (Leiden University Medical Center, Leiden, The Netherlands, and Netherlands Cancer Institute, Antonie van Leeuwenhoek Hospital, Amsterdam, The Netherlands), informed consent was obtained from all patients or parents for performance of radiologic studies and analysis of clinical data anonymously. The institutional review board approved the study protocol.

MR imaging

MR imaging was performed with either of two 1.5-T MR imaging systems (Philips Medical Systems, Best, Netherlands [maximum gradient strength of 23 mT/m]; Siemens Medical Systems, Erlangen, Germany [maximum gradient strength of 25

mT/m]) and similar pulse sequences. Hereafter, these systems will be referred to as MR imaging system A and B, respectively. Either a body or surface coil was used, depending on the location and size of the lesion. The body coil was used in retroperitoneal and abdominal lesions, whereas extremity lesions were imaged by using a surface coil, except for a few very large tumors.

Standard MR imaging was performed with T1-weighted [repetition time (TR) msec/echo time (TE) msec: 244-800/7-25, echo train length (ETL): 5] fast spin echo sequences and fat-suppressed T2-weighted [TR/TE: 1800-5929/20-99, ETL 9] fast spin echo sequences. A dynamic contrast-enhanced MR imaging sequence was performed after these sequences.

Dynamic MR imaging was performed using a T1-weighted gradient-echo sequence. With MR system A, we used a turbo field echo (TFE) sequence with TR/TE 5.4 msec/1.4 msec, flip angle 20°, non-selective inversion preparatory pulse, preparatory pulse delay time 165 msec, number of excitations 1, matrix size 256x102, field of view 300-400 mm, section thickness 5-8 mm. With MR system B, we used a fast low angle shot (FLASH) sequence with TR/TE 29.2 msec/1.4 msec, flip angle 30°, number of excitations 1, matrix size 128x95, field of view 400 mm, section thickness 5-10 mm. A series of 60-100 of these T1-weighted gradient-echo sequences were obtained during the first pass of the bolus gadopentetate dimeglumine with a time interval, or temporal resolution, of 3 seconds during at least the first 84 seconds. Total scanning time was 5 minutes. A power injector (Spectris; Medrad, Indianola, Pa) with an injection flow rate of 2 ml per second was used to start the intravenous administration of 0.1 mmol/kg body weight of gadopentetate dimeglumine (Magnevist, Schering, Berlin, Germany; Prohance, Bracco, Milano, Italy) followed by 20 ml saline flush. Bolus injection was initiated 5 seconds after start of data acquisition. For dynamic imaging, one of the authors (CSPvR) selected the plane and location that showed to best advantage the tumor and an artery within the same field of view by using the nonenhanced T1- and T2-weighted images. The second pre-contrast dynamic image was subtracted (CSPvR) from all dynamic contrast-enhanced MR images as follows: manually, with the computer of MR imaging system B, and automatically by using commercially available software with MR imaging system A. Regions of interest that were drawn freehandedly were selected by one of the authors without knowledge of the histopathologic findings in the earliest contrast enhancing part of the lesion and in the artery within the same field of view. Regions of interest had a total pixel area of approximately 80-200 mm2 for the artery and 100-400 mm^2 for the lesions. Time-

signal intensity curves, generated by using commercially available software on computers of both systems, were documented on hard copies for independent reading.

The T1-weighted fast spin echo sequence was repeated with fat suppression after performance of the dynamic sequence in at least two planes within 5 to 10 minutes of administration of the contrast-agent (static contrast-enhanced MR images).

Image interpretation

On nonenhanced MR images we evaluated lesion size, margins, peritumoral edema (ill defined zone of high signal intensity on T2-weighted MR images that extended from the well-defined margin of the lesion into the surrounding tissues) (14;29), signal intensity characteristics, homogeneity, presence or absence of hemorrhage (high signal intensity on T1 and low or high signal intensity on T2-weighted MR images, not isointense to fat), and involvement of bone (extension of tumor into cortex), joint and neurovascular bundle (encasement if surrounded with tumor for at least half the structure's circumference and obliteration of fat plane) (30).

Figure 1

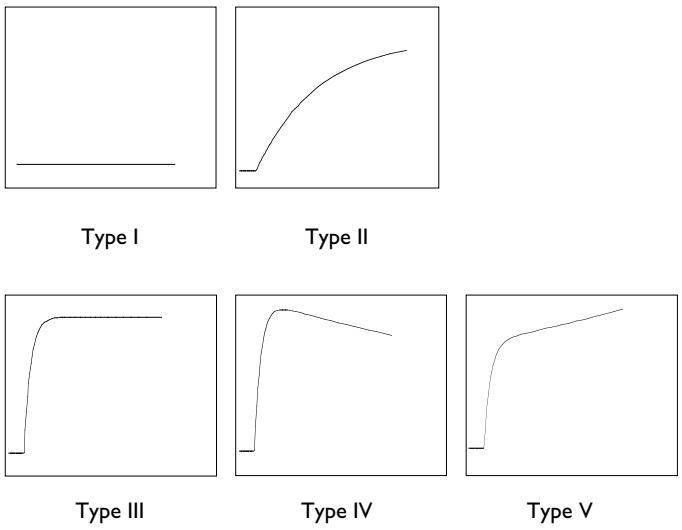

Figure 1

Diagram shows classification for subjective assessment of time-signal intensity curves: type I, no enhancement; type II, gradual increase of enhancement; type III, rapid initial enhancement followed by a plateau phase; type IV, rapid initial enhancement followed by a washout phase; and type V, rapid initial enhancement followed by sustained late enhancement.

We subjectively evaluated three dynamic contrast-enhanced MR parameters (25-27): start of tumor enhancement (time interval between start of arterial and tumor enhancement), spatial pattern of enhancement, and progression of tumor enhancement. An arbitrary threshold of six seconds was chosen for start of tumor enhancement based on results with the first pass of the contrast-agent after injection of 2 ml per second in extremity musculoskeletal tumors (25;26). The progression of tumor enhancement was subjectively classified according to the shape of the time-signal intensity curve (Figure 1) (31).

After intravenous administration of gadopentetate dimeglumine, we evaluated the morphology of late (5-10 minutes) enhancement on the static T1-weighted MR images. Intralesional iso- or hypointense signal intensity relative to muscle on T1-weighted MR images, high signal intensity on T2-weighted MR images, and no contrast enhancement on static contrast-enhanced MR images were assumed to be liquefaction.

Two experienced musculoskeletal radiologists (M.J.A.G., 13 years of experience; J.L.B., 20 years of experience), one at each participating institution, who were blinded with regard to the diagnosis, clinical history and the results of other imaging studies, independently interpreted all MR images from both institutions. All MR images were randomized as two data sets. The nonenhanced MR images were analyzed first. Subsequently, static and dynamic contrast-enhanced MR images, including the time-signal intensity curves, were added. On both data sets, each observer evaluated the specific MR parameters and diagnosed the lesion as benign or malignant with a five-point confidence rating (1= definitely benign, 2= uncertain benign, 3= undetermined, 4= uncertain malignant, 5= definitely malignant).

Statistical analysis

The frequency distribution of the individual MR imaging parameters in the benign tumor group was compared with that in the malignant tumor group by using the chi-square test. A P value of < 0.05 was considered to indicate a significant difference. Interobserver agreement of the individual MR parameters was determined by means of kappa (κ)-analysis; a κ value of less than 0.40 was considered to represent poor agreement; that equal or greater than 0.40 and less than 0.60, moderate agreement; that equal to or greater than 0.60 and less than 0.80, good agreement; and that equal to or greater than 0.80 excellent agreement.

Multivariate logistic regression analysis was used to identify the best combination of MR imaging parameters that might be predictive for malignancy. The

analysis was performed for both observers independently and was started by entering the nonenhanced MR imaging parameters (model 1). Subsequently, static contrast-enhanced MR parameters were added (model 2), and, finally dynamic contrast-enhanced MR parameters were added (model 3). Final selection of multivariate predictors (model 4) was determined with stepwise analysis as a backward-stepping procedure that was based on a likelihood ratio test, with a P value greater than 0.10 used for exclusion from the model. The regression coefficient, b, of the selected variables of model 4 provided an estimate of the extent to which each parameter contributed to the diagnostic accuracy. The diagnostic performance of the four regression models was quantified with the model deviance and was compared by using a likelihood ratio test. As a model's ability to predict malignancy improves, the deviance decreases. Subsequently, poorly fitting models have higher deviance. The incremental value of static contrast-enhanced MR parameters and a combination of static and dynamic contrast-enhanced MR parameters relative to the value of nonenhanced MR imaging parameters in the differentiation between benign and malignant soft tissue lesions was evaluated by using this method. The multivariate logistic regression analysis was repeated for the extremity soft tissue lesions after exclusion of retroperitoneal, abdominal, chest wall, and soft tissue lesions located in the head or neck region. Model fit was evaluated by means of the Hosmer-Lemeshow goodness-of-fit test (32).

For both observers, receiver operating characteristics curves of the subjective MR diagnosis obtained at nonenhanced, and combined nonenhanced with contrast-enhanced MR images, including static and dynamic contrast-enhanced MR imaging parameters, were constructed. The area under each receiver operating characteristic curve, a measure for diagnostic accuracy in the prediction of the benign or malignant nature, was calculated, and the significance of differences between both tests and both observers was assessed by using a univariate z-score test (33;34).

Results of subjective MR imaging diagnosis were analyzed for sensitivity and specificity with a confidence rating of uncertain benign, undetermined, uncertain malignant and definitely malignant as positive readings requiring histological biopsy and with a confidence rating of definitely benign as a negative reading.

Data analysis was performed with statistical software (SPSS for Windows, version 10.0; SPSS, Chicago, Ill). Receiver operating characteristic analysis was performed by using other software (ROCKIT; C.E. Metz. MD, University of Chicago, Ill).

Power calculations that were based on data from previous studies were used to determine that a sample size of 70 malignant and 70 benign soft tissue lesions was sufficient to detect a significant difference in MR imaging sensitivity and specificity with a 75% power at a P value of 0.05 (16-22).

RESULTS

Diagnoses

Seventy-three malignant soft tissue masses (including six lesions that recurrenced after a disease-free interval of 16 months to 10 years, mean 4.4 years) and 67 benign soft tissue masses formed the basis of the study. All 73 malignant tumors and 56 of the 67 benign tumors were histologically confirmed. The remaining 11 benign soft tissue tumors were considered benign at clinical follow-up at each 6-months interval and with no growth for at least 2 years. The final diagnoses that were based on MR imaging and clinical data include four cases of lipoma, two of cysts, one of fat necrosis, and one of elastofibroma. Three vascular malformations were diagnosed after additional angiography and/or venography as part of the diagnostic work-up for vascular anomalies.

Cases of histologically proved benign masses included 10 of lipoma, 10 of desmoid-type fibromatosis, five of vascular anomaly, five of schwannoma, four of cysts (one each of Baker cyst, synovial cyst, Echinococcus cyst and epidermoid cyst), four of ganglion, three of myofibroblastic proliferation (two of nodular fasciitis and one of myositis ossificans), two of pigmented villonodular synovitis, and one each of pleomorphic hyalinising angiectatic tumor, abscess, bursitis, giant cell tumor of the tendon sheath, rheumatoid tophus, tophaceous gout, thrombosed vein, synovial chondromatosis, foreign body granuloma, ganglionneuroma, leiomyoma, myxoma, and lymph node containing Toxoplasmosa gondii organisms.

Cases of malignancy included 22 of liposarcomas (10 atypical lipomatous, four myxoid round cell, three dedifferentiated, three pleiomorphic, and two sclerosing tumors), 12 of high-grade sarcomas not otherwise specified, nine of soft tissue metastasis (without known primary malignancy), five of myxofibrosarcoma, five of leiomyosarcoma, five of malignant peripheral nerve sheath sarcoma, four of myofibroblastic sarcoma, two of embryonal rhabdomyosarcoma, two of angiosarcoma, and one each of alveolar soft part sarcoma, synovial sarcoma, clear cell sarcoma, gastrointestinal stroma cell tumor, epithelioid sarcoma, soft tissue localization of lymphoma, and radiation-induced fibrosarcoma.

Lesions were located in the lower extremity (n=70), upper extremity (n=41), abdomen (n=9), retroperitoneum (n=8), chest wall (n=7), and head or neck region (n=5).

Frequency distribution and interobserver agreement of individual MR imaging parameters

Table 1 and 2 list the data for frequency distribution of nonenhanced MR imaging parameters (Table 1) and static and dynamic contrast-enhanced MR imaging parameters (Table 2), correlation of these parameters with final diagnosis (benign or malignant tumors) of observer 1, as well as agreement between observer 1 and 2. For both observers, lesion size, neurovascular involvement, presence of edema, liquefaction, and all three dynamic contrast-enhanced MR imaging parameters were correlated ($P < 0.05$) with the diagnosis of malignancy.

All static and dynamic contrast-enhanced MR imaging parameters had good to excellent interobserver agreement. On nonenhanced MR imaging, only size (largest diameter), presence of edema, signal intensity on T1- and T2-weighted MR images, and bone and joint involvement had good to excellent interobserver agreement. The other nonenhanced MR parameters had moderate to poor interobserver agreement.

Table 1

Frequency distribution and correlation with final diagnosis of nonenhanced MR imaging parameters for observer 1 and interobserver agreement

MR imaging parameter	Benign tumors (n= 67)	Malignant tumors (n= 73)	P value	κ value**
Largest diameter (cm)*			< 0.001	1.0
< 5 cm	35	15		
5-10 cm	26	26		
> 10 cm	6	32		
Margins			0.21	0.50
well defined	39	37		
partially defined	15	26		
ill defined	13	10		
infiltrating	0	0		
Peritumoral edema*			0.007	0.62
not present	39	26		
present	28	47		

MR imaging parameter	Benign tumors (n= 67)	Malignant tumors (n= 73)	P value	κ value**
T1 signal intensity			0.42	0.65
lower or equal to muscle	33	37		
slightly higher than muscle	15	16		
between muscle and fat	3	8		
higher or equal to fat	16	12		
T2 signal intensity			0.10	0.73
lower or equal to muscle	11	6		
slightly higher than muscle	8	4		
higher than muscle	48	63		
T1 homogeneity				
100% homogeneous	27	22		
<25% of mass inhomogeneous	27	27		
25-50% inhomogeneous	5	8		
> 50% inhomogeneous	8	16		
T2 homogeneity			0.003	0.41
100% homogeneous	22	7		
<25% of mass inhomogeneous	20	23		
25-50% inhomogeneous	7	18		
> 50% inhomogeneous	18	25		
Bone			0.05	0.76
normal	60	59		
erosion/ periosteal reaction	2	0		
invasion	5	14		
Neurovascular*			0.006	0.51
not involved	51	43		
contact/ displacement	13	13		
encased	3	17		
Joint			0.24	0.77
not involved	55	65		
involved	12	8		
Hemorrhage			0.04	0.33
not present	59	54		
present	8	19		

** A κ value (interobserver agreement) less than 0.40 represented poor agreement; that equal to or greater than 0.40 and less than 0.60, moderate agreement; that equal to or greater than 0.60 and less than 0.80, good agreement; and that equal to or greater than 0.80 excellent agreement.

* Indicates MR imaging parameter with significant P values for both observers

Table 2

Frequency distribution and correlation with final diagnosis of static and dynamic contrast-enhanced MR imaging parameters for observer 1 and interobserver agreement

MR imaging parameter	Benign tumors (n= 67)	Malignant tumors (n= 73)	P value	κ value**
Static enhancement				
Pattern of enhancement			0.002	0.70
diffuse	18	11		
peripheral	7	7		
inhomogeneous	30	53		
absence	12	2		
Liquefaction*			< 0.001	0.60
not present	54	27		
present	13	46		
Dynamic enhancement				
Start of enhancement*			< 0.001	0.88
≤ 6 sec.	31	59		
> 6 sec.	36	14		
Pattern of enhancement*			< 0.001	0.72
diffuse	18	9		
peripheral	13	40		
inhomogeneous	16	15		
absence	20	9		
Progression of enhancement*			0.001	0.70
I (absence)	19	9		
II (gradual increase)	16	4		
III (rapid plateau)	16	32		
IV (rapid washout)	11	17		
V (rapid sustained increase)	5	11		

** A κ value (interobserver agreement) less than 0.40 represented poor agreement; that equal to or greater than 0.40 and less than 0.60, moderate agreement; that equal to or greater than 0.60 and less than 0.80, good agreement; and that equal to or greater than 0.80 excellent agreement.

* Indicates MR imaging parameter with significant P values for both observers

Combination of MR imaging parameters for all soft tissue lesions

The diagnostic performance, quantified with the model deviance, and the resulting sensitivity and specificity with regard to malignancy of the individual logistic regression models were not significantly different between the two observers. Results of observer 1 and 2 are represented in Table 3. Logistic regression model 3, based on the combination of nonenhanced, static and dynamic contrast-enhanced MR imaging parameters, had significantly lower model deviance than did logistic regression model 1 and model 2, and this result led to the highest ability to predict malignancy with a sensitivity of 82% and 84%, with specificity of 78% and 82% for observer 1 and 2, respectively (Figure 2-4). Stepwise multivariate logistic regression analysis (model 4, Table 3) with all evaluated MR imaging parameters revealed that only three of 16 parameters were significant predictors of malignancy for observer 1. The same three parameters were significant predictors for observer 2, but an additional set of parameters was also significant for this observer. The discriminating parameters of observer 1 were presence of liquefaction (b=1.51, standard error (se)=0.44), start of dynamic enhancement (b=1.22, se=0.44), and lesion size (b=1.10, se=0.29). The discriminating parameters of observer 2 were presence of liquefaction (b=1.96, se=0.70), start of dynamic enhancement (b=1.90, se=0.66), lesion size (b=1.37, se=0.36), and, in addition, presence of edema (b=1.08, se=0.56), signal intensity on T2-weighted MR images (b=0.79, se=0.43) and on T1-weighted MR images (b=0.74, se=0.26), and homogeneity on T2-weighted MR images (b=-0.60, se=0.26). The predictive probabilities of the models for observer 1 and 2 (model 4) were not significantly different (P = 0.99).

The Hosmer-Lemeshow goodness-of-fit test results were not significantly different for each model, and these results indicate that all the models were adequately fitted.

Combination of MR imaging parameters for extremity lesions only

For the extremity lesions, logistic regression model 3, which was based on the combination of nonenhanced, static and dynamic contrast-enhanced MR imaging parameters, had significantly lower model deviance than did logistic regression model 1. Model deviance of model 3 was also lower than that of model 2 (no significant difference for observer 1, P < 0.005 for observer 2), and this finding resulted in the highest ability to predict malignancy with a sensitivity of 70% and 82% and with a specificity of 81% and 83% for observer 1 and 2, respectively. Results of observer

Table 3

Logistic regression models of the MR imaging parameters of observer 1 and 2: analysis of all 140 soft tissue lesions

Model		Deviance		No. of MR imaging parameters		Sensitivity (n=73)*		Specificity (n-67)*	
		obs. 1	obs. 2	obs. 1	obs. 2	obs. 1	obs. 2	obs. 1	obs. 2
1	Standard nonenhanced MR imaging parameters	150.95	134.04	11	11	69 (50)	77 (56)	73 (49)	76 (51)
2	Standard nonenhanced combined withstatic contrast-enhanced MR imagingparameters	139.84	125.96	13	13	74 (54)	80 (58)	78 (52)	79 (53)
3	Standard nonenhanced combined withstatic and dynamic contrast-enhancedMR imaging parameters	131.26	112.36	16	16	82 (60)	84 (61)	78 (52)	82 (55)
4	Stepwise logistic regression analysis of model 3	140.22	120.43	3**	7***	75 (55)	78 (57)	66 (44)	82 (55)

Note.- Differences between models 1 and 2 ($P < 0.005$ for observer 1, $P < 0.003$ for observer 2), model 2 and 3 ($P < 0.05$ for observer 1, $P < 0.005$ for observer 2), and models 1 and 3 ($P < 0.005$ for observer 1, $P < 0.001$ for observer 2) were all significant for both observers.

* Numbers are percentages. Numbers in parentheses were used to calculate the percentages.

** MR imaging parameters included presence of liquefaction, start of dynamic enhancement, and lesion size

*** MR imaging parameters included presence of liquefaction, start of dynamic enhancement, lesion size, presence of edema, signal intensity on T2 and T1-weighted MR images and homogeneity on T2-weighted MR images

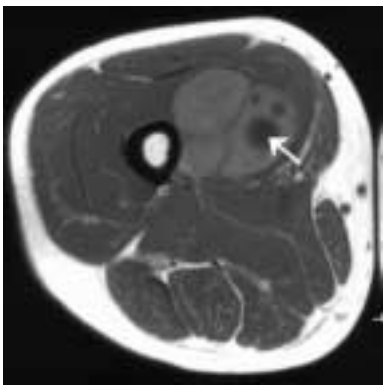

Figure 2a

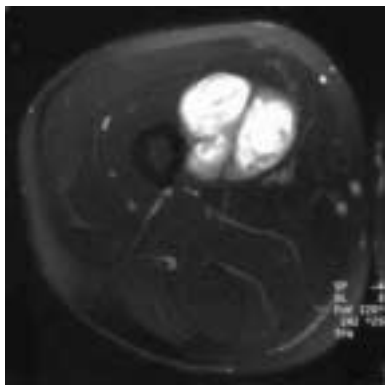

Figure 2b

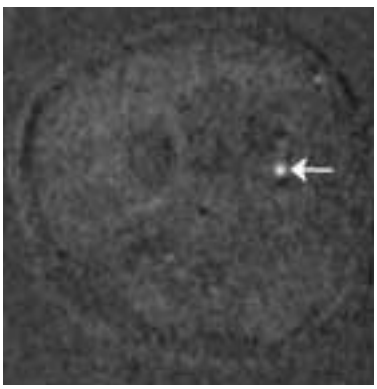

Figure 2c

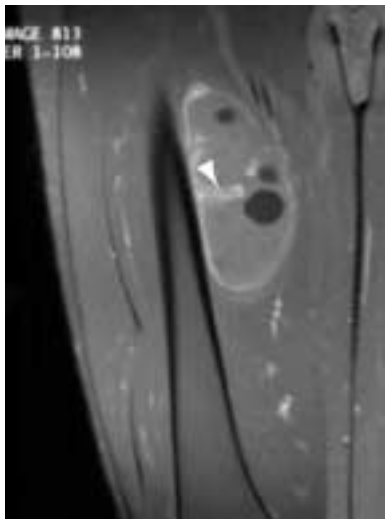

Figure 2d

Figure 2

a Transverse T1-weighted MR image (513/12) of an intramuscular soft tissue mass in the upper part of the right leg in a 42-year-old man demonstrates cystic parts (arrow).

b Corresponding transverse fat suppressed T2-weighted MR image (3508/99) shows lobulated soft tissue mass with heterogeneous high signal intensity.

c Subtraction dynamic contrast-enhanced MR image (29.2/1.4) obtained at the same level as a and b, 30 s after arrival of the bolus of gadopentetate dimeglumine in femoral artery (arrow). Absence of early dynamic enhancement suggests a benign lesion.

d Coronal static contrast-enhanced MR image (451/12) depicts peripheral and septal (capsular) enhancement (arrowhead). Histologic examination after core-needle biopsy showed Echinococcus cyst.

1 and 2 are represented in Table 4. For both observers, the same three parameters (liquefaction, start of dynamic enhancement and lesion size) were significant predictors of malignancy. Compared with the entire study population, the additional set of parameters for observer 2 was smaller and included signal intensity and homogeneity on T1-weighted MR images for the extremity lesions only.

Lesion characterization and confidence of subjective MR imaging diagnosis

The receiver operating characteristic curves of the confidence of subjective MR imaging diagnosis of both observers are illustrated in Figure 5. For both observers, the area under the receiver operating characteristic curve values for the combined assessment of nonenhanced and contrast-enhanced MR image sets, including static and dynamic contrast-enhanced MR imaging parameters (area under the receiver operating characteristic curve, 0.96 for observer 1 and 0.92 for observer 2), were significantly larger compared with the values observed for nonenhanced MR imaging alone (area under the receiver operating characteristic curve, 0.90, $P < 0.001$ for observer 1; area under the receiver operating characteristic curve, 0.88, $P = 0.03$ for observer 2). The area under the receiver operating characteristic curve values were not significantly different between observer 1 and 2.

Counting a subjective MR imaging diagnosis classified according to our five-point confidence rating scale of uncertain benign, undetermined, uncertain malignant or definitely malignant as a positive reading requiring histologic biopsy and counting a rating of definitely benign as a negative reading, with nonenhanced MR imaging, sensitivity was 99% (72 of 73) and 100% (73 of 73) and specificity was 19% (13 of 67)(95% confidence interval: 13%, 25%) and 13% (nine of 67)(95% confidence interval: 7%,19%) for observer 1 and 2, respectively. At contrast-enhanced MR imaging sensitivity remained very high (99% [72 of 73] for both observers), with a significant increase of specificity to 48% (32 of 67)(95% confidence interval, 40%, 56%) and 36% (24 of 67)(95% confidence interval, 28%, 44%) for observer 1 and 2, respectively. Increase in specificity was significant for both observers, as demonstrated by the absence of overlap at the 95% confidence intervals.

Table 4

Logistic regression models of MR imaging parameters for observer 1 and 2: analysis of 111 extremity soft tissue lesions

Model		Deviance		No. of MR imaging parameters		Sensitivity (n=54)*		Specificity (n-57)*	
		obs. 1	obs. 2	obs. 1	obs. 2	obs. 1	obs. 2	obs. 1	obs. 2
1	Standard nonenhanced MR imaging parameters	122.71	115.28	11	11	66 (36)	69 (37)	74 (42)	77 (44)
2	Standard nonenhanced combined with static contrast-enhanced MR imaging parameters	115.49	107.13	13	13	70 (38)	74 (40)	77 (44)	81 (46)
3	Standard nonenhanced combined with static and dynamic contrast-enhanced MR imaging parameters	108.73	93.69	16	16	70 (38)	82 (44)	81 (46)	83 (47)
4	Stepwise logistic regression analysis of model 3	118.27	103.78	3**	5***	63 (34)	74 (40)	81 (46)	86 (49)

Note.- Differences between models 1 and 2 ($P < 0.05$ for observer 1, $P < 0.025$ for observer 2), and between models 1 and 3 ($P < 0.025$ for observer 1, $P < 0.001$ for observer 2) were significant. Difference between models 2 and 3 (not significant for observer 1, $P < 0.005$ for observer 2) were only significant for observer 2.

* Numbers are percentages. Numbers in parentheses were used to calculate the percentages.

** MR imaging parameters included presence of liquefaction, start of dynamic enhancement, and lesion size

** MR imaging parameters included presence of liquefaction, start of dynamic enhancement, lesion size, and signal intensity and homogeneity on T1-weighted MR images

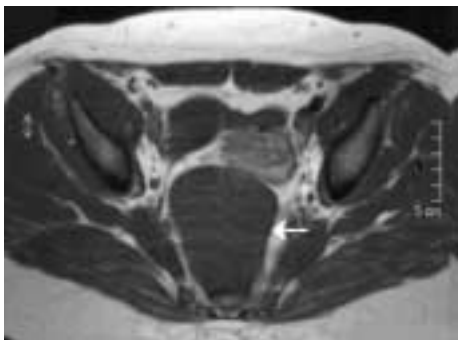

Figure 3a

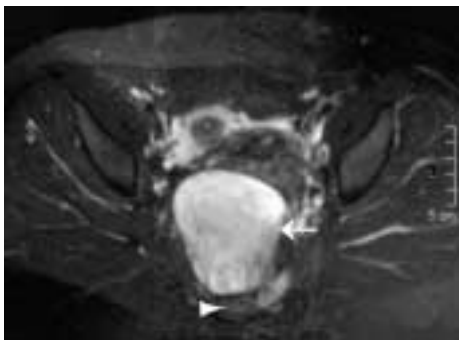

Figure 3b

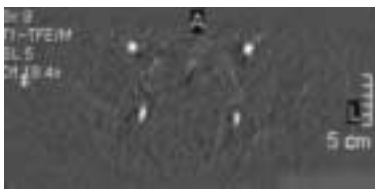

Figure 3c

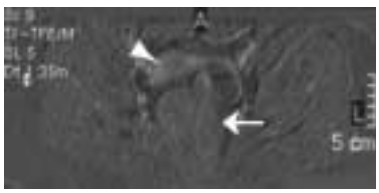

Figure 3d

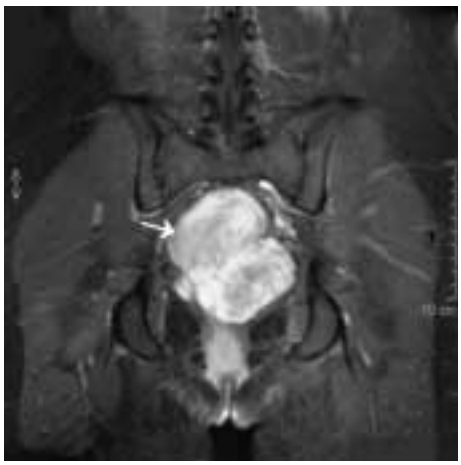

Figure 3e

Figure 3

a Transverse T1-weighted MR image (550/12) of a pelvic soft tissue mass (arrow).

b Corresponding transverse fat suppressed T2-weighted MR image (3712/80) revealed a large soft tissue mass (arrow) in the pelvis in close relation to the sacrum (arrowhead) but without osseous involvement.

c Transverse subtraction dynamic contrast-enhanced MR image (5.4/1.4) obtained 12 mm inferior to the level of a and b. Arrival of the bolus of gadopentetate dimeglumine in the internal and external iliac arteries is demonstrated.

d Transverse subtraction dynamic contrast-enhanced MR image(5.4/1.4) obtained more than 1 minute after arrival of the contrast agent bolus in the arteries. No enhancement is seen in the tumor (arrow), which suggests a benign lesion. Uterine body also enhances (arrowhead).

e Coronal static contrast-enhanced MR image (550/12) demonstrates intense enhancement (arrow). Note that absence of early enhancement on the dynamic contrast-enhanced MR images does not preclude intense enhancement on the static (delayed) contrast-enhanced MR images. Histologic examination after core-needle biopsy revealed ganglioneuroma.

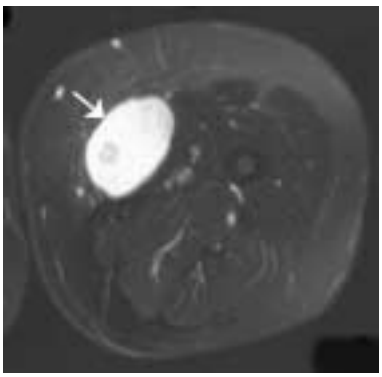

Figure 4a

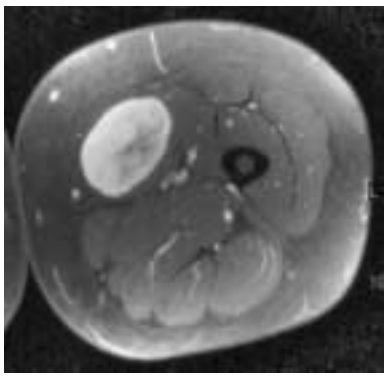

Figure4b

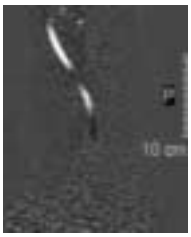

Figure 4c

Figure 4d

Figure 4e

Figure 4

a Transverse T2-weighted fat suppressed MR image (3718/80) MR image in a 57-year-old woman with a myxoid round cell liposarcoma in the upper part of the left leg (arrow).
b Corresponding static contrast-enhanced MR image MR image (550/7).
c,d,e Sagittal subtraction dynamic contrast-enhanced MR images (5.4/1.4) obtained at the same level.
c Arrival of the bolus of gadopentetate dimeglumine in femoral artery.
d Dynamic subtraction MR image obtained 6 s later than c shows early enhancement of the tumor (arrow), which is consistent with malignancy.
e Dynamic subtraction MR image obtained 30 s later than c shows more intense enhancement of the tumor.

DISCUSSION

Contrast-enhanced MR imaging improved diagnostic performance relative to nonenhanced MR imaging in our patients. All patients had a soft tissue mass at presentation at a tertiary referral center; the mass was clinically suspected to be a sarcoma. The receiver operating characteristic curves displaying subjective MR imaging diagnoses of all soft tissue lesions revealed the value of contrast-enhanced MR imaging. The confidence of subjective MR imaging diagnosis (benign or malignant lesions) significantly improved by addition of contrast-enhanced MR imaging, including morphologic and dynamic MR imaging parameters, relative to nonenhanced MR imaging alone.

Figure 5

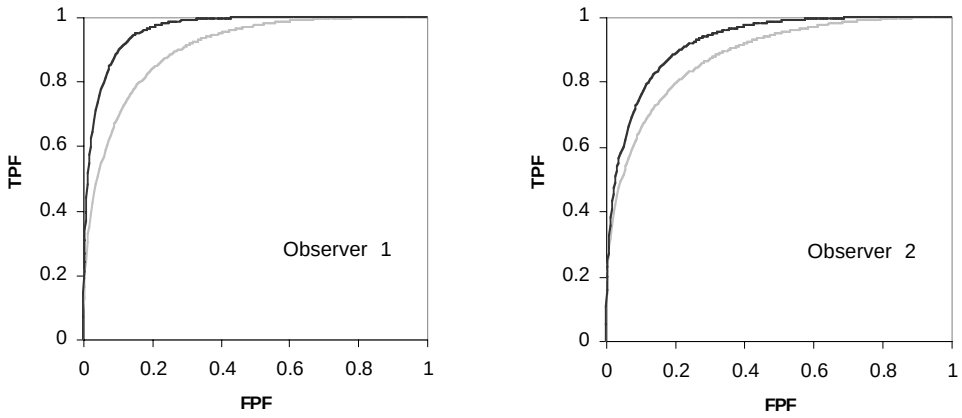

Graphs show receiver operating characteristic curves of observers 1 and 2. Graphs illustrate comparison between nonenhanced MR imaging (gray line) and combination of nonenhanced and contrast-enhanced MR imaging, including morphologic and dynamic contrast-enhanced MR imaging parameters (black line), in the confidence of subjective diagnosis of soft tissue lesions. With contrast-enhanced MR images, lesion characterization was significantly improved ($P < 0.001$ and $P = 0.03$ for observer 1 and 2, respectively). Readings between both observers were not significantly different. FPF: false positive fraction, TFP: true positive fraction.

An individual MR imaging parameter or a combination of MR imaging parameters will have practical application in the differentiation of benign from malignant soft tissue masses if it is significantly associated with the benign or malignant nature of the lesion and has high interobserver agreement. Our univariate analysis demonstrated that six of 16 parameters fulfilled these criteria. Seven of 16 parameters were significantly associated with the benign or malignant nature of the lesion. Four of these seven were enhancement parameters. Nonenhanced MR imaging parameters that favored malignancy were as follows: large lesion size, edema and neurovascular involvement. Contrast-enhanced MR imaging parameters that favored malignancy were liquefaction, early dynamic enhancement (within 6 s after arterial enhancement), peripheral or inhomogeneous dynamic enhancement, and rapid initial dynamic enhancement followed by a plateau or washout phase. With the exception of neurovascular involvement (moderate interobserver agreement), these parameters had good to excellent interobserver agreement.

For all soft tissue lesions, multivariate logistic regression analysis supported by

model deviance demonstrated that sensitivity and specificity increased significantly for both observers when static contrast-enhanced MR imaging (model 2) was added to nonenhanced MR imaging (model 1). For both observers, sensitivity increased significantly, with stable specificity for observer 1 and increase of specificity for observer 2, when dynamic MR imaging (model 3) was added to static contrast-enhanced MR imaging (model 2). For both observers, the most important predictors of malignancy (model 4) were presence of liquefaction, early start of dynamic enhancement, and large lesion size. The two most significant parameters of these three, liquefaction and start of dynamic enhancement, were obtained with use of gadopentetate dimeglumine. For observer 2, four less important (lower b values) parameters, edema, signal intensity on T1- and on T2-weighted MR images and homogeneity on T2-weighted MR images, were added during the final steps of the backward-stepwise regression analysis. Not surprisingly, for both observers, the κ-values of the three most significant parameters were good to excellent.

Our results, indicating that large lesion size and the presence of liquefaction are highly suggestive for malignancy, are consistent with the results of De Schepper et al. (18). Early dynamic enhancement has been described by Van der Woude et al. (25) and Verstraete et al. (26;35) as an important MR parameter to indicate the presence of musculoskeletal sarcoma. Van der Woude et al. (25) found a positive predictive value of 71%, which is slightly larger than our positive predictive value of 66% for both observers. Verstraete et al. (26;35) did not find this parameter very useful because of considerable overlap between benign and malignant lesions, despite the significant differences between the two groups.

Although benign soft tissue lesions at all sites outnumber their malignant counterparts, in the retroperitoneum, sarcomas are at least as prevalent as benign soft tissue lesions (36). Therefore, we repeated the logistic regression analysis for only extremity lesions. Regression analysis supported by model deviance (Table 4) demonstrated the same significant increase in sensitivity and specificity for both observers when static contrast-enhanced MR parameters (model 2) were added to nonenhanced MR imaging parameters (model 1). For observer 2, a further increase in sensitivity and specificity was reached when dynamic MR imaging parameters (model 3) were added to static contrast-enhanced MR imaging parameters (model 2). However, for observer 1, addition of dynamic MR imaging parameters (model 3) did not significantly improve diagnostic performance compared with the combination of nonenhanced and static contrast-enhanced MR imaging parameters (model 2).

Presence of liquefaction, early start of dynamic enhancement, and large lesion size were the most discriminating parameters for both observers.

When one assesses the diagnostic MR criteria for differentiation between benign and malignant soft tissue lesions, it is important to stress that histopathologic findings remain the gold standard. In our practice, biopsy is performed on all malignant soft tissue tumors, also including those that are definitely malignant on MR imaging, to obtain a specific histopathologic diagnosis to decide what type of subsequent therapy is required. However, in our opinion, soft tissue lesions in which the observer is highly confident of the benign diagnosis on MR imaging (our confidence rating of definitely benign) may not require histologic biopsy. As demonstrated by the subjective analysis and multivariate analysis of the extremity lesions, addition of contrast-enhanced MR imaging sequences did significantly increase specificity for both observers, with sensitivity remaining excellent. The histological diagnoses in which both observers became highly confident of the benign diagnosis after addition of contrast-enhanced MR imaging were predominantly those of lipoma, ganglion, cyst, vascular anomaly, and desmoid-type fibromatosis. Subsequently, the use of gadopentetate dimeglumine may have an effect on clinical treatment because the number of histologic biopsies performed in the benign group is reduced. Accurate MR imaging diagnosis may also influence patient care when MR findings contradict biopsy results. This becomes increasingly important since closed core-needle biopsy often is used instead of incisional biopsy as the preferred method (37;38).

There is controversy in regard to the routine use of contrast agents (either static or dynamic contrast-enhanced MR imaging) in the diagnosis of musculoskeletal neoplasms (16-28;39;40). We realize that time and money may prohibit the routine use of either or both of these techniques in routine clinical practice. However, the superior diagnostic performance of contrast-enhanced MR imaging can be used not only to improve diagnosis of benign lesions but also to improve detection of malignancy because of increased sensitivity after addition of gadopentetate dimeglumine. In routine clinical practice, synovial sarcoma is frequently misinterpreted as benign on nonenhanced MR imaging, perhaps because of its often small size, well-defined margins and slow progression (11;41). However, these sarcomas will demonstrate early enhancement at dynamic contrast-enhanced MR imaging (42). Enhancement characteristics may, therefore, raise a red flag in benign appearing lesions and allow less experienced radiologists to target lesions that need further work-up in a referral center.

A criticism of our study is the unavoidable case-selection bias, because all patients had soft tissue lesions that were considered to be of sufficient concern at clinical evaluation to merit assessment, at two tertiary referral hospitals, for bone and soft tissue sarcomas. However, despite this selection bias, nearly half (67 of 140) of the patients had benign soft tissue lesions. Another limitation of our study was the verification bias because 11 of 67 benign lesions were not confirmed at biopsy. The follow-up period of 2 years in these patients without biopsy was, in our opinion, long enough to exclude the possibility that any of these lesions eventually could prove to be malignant. Another limitation of this study was that data were obtained with two MR imaging systems as a consequence of the bicenter nature of the study.

In conclusion, for soft tissue tumors, combined nonenhanced, static and dynamic contrast-enhanced MR imaging demonstrated the best diagnostic performance in predicting malignancy, compared with nonenhanced MR images alone and compared with combined nonenhanced MR imaging and static contrast-enhanced MR imaging. We advocate use of this approach when biopsy can be avoided because of confident diagnosis in selected cases. A second reason to use dynamic contrast-enhanced MR imaging is to create a safety net, because increased diagnostic performance allows identification of sarcoma that has benign morphologic features at nonenhanced MR imaging.

REFERENCES

1 .Parker SL, Tong T, Bolden S, Wingo PA. Cancer statistics, 1996. CA Cancer J Clin 1996; 46:5-27.
2. Fletcher CD, Unni KK, Mertens F (eds.): World Health Organization Classification of Tumours. Pathology and Genetics of Tumours of Soft Tissue and Bone. IARC Press: Lyon 2002.
3. Kransdorf MJ. Benign soft-tissue tumors in a large referral population: distribution of specific diagnoses by age, sex, and location. AJR Am J Roentgenol 1995; 164:395-402.
4. van Glabbeke M, van Oosterom AT, Oosterhuis JW, et al. Prognostic factors for the outcome of chemotherapy in advanced soft tissue sarcoma: an analysis of 2,185 patients treated with anthracycline-containing first-line regimens--a European Organization for Research and Treatment of Cancer Soft Tissue and Bone Sarcoma Group Study. J Clin Oncol 1999; 17:150-157.
5. Patel SR, Vadhan-Raj S, Burgess MA, et al. Results of two consecutive trials of dose-intensive chemotherapy with doxorubicin and ifosfamide in patients with sarcomas. Am J Clin Oncol 1998; 21:317-321.
6. Chang AE, Matory YL, Dwyer AJ, et al. Magnetic resonance imaging versus computed tomography in the evaluation of soft tissue tumors of the extremities. Ann Surg 1987; 205:340-348.
7. Sundaram M, McGuire MH, Herbold DR. Magnetic resonance imaging of soft tissue masses: an evaluation of fifty-three histologically proven tumors. Magn Reson Imaging 1988; 6:237-248.
8. Totty WG, Murphy WA, Lee JK. Soft-tissue tumors: MR imaging. Radiology 1986; 160:135-141.
9. Rubin DA, Kneeland JB. MR imaging of the musculoskeletal system: technical considerations for enhancing image quality and diagnostic yield. AJR Am J Roentgenol 1994; 163:1155-1163.
10. Kransdorf MJ, Jelinek JS, Moser RP Jr., et al. Soft-tissue masses: diagnosis using MR imaging. AJR Am J Roentgenol 1989; 153:541-547.
11. Berquist TH, Ehman RL, King BF, Hodgman CG, Ilstrup DM. Value of MR imaging in differentiating benign from malignant soft-tissue masses: study of 95 lesions. AJR Am J Roentgenol 1990; 155:1251-1255.
12. Crim JR, Seeger LL, Yao L, Chandnani V, Eckardt JJ. Diagnosis of soft-tissue masses with MR imaging: can benign masses be differentiated from malignant ones? Radiology 1992; 185:581-586.
13. Petasnick JP, Turner DA, Charters JR, Gitelis S, Zacharias CE. Soft-tissue masses of the locomotor system: comparison of MR imaging with CT. Radiology 1986; 160:125-133.
14. Moulton JS, Blebea JS, Dunco DM, Braley SE, Bisset GS III, Emery KH. MR imaging of soft-tissue masses: diagnostic efficacy and value of distinguishing between benign and malignant lesions. AJR Am J Roentgenol 1995; 164:1191-1199.
15. Kransdorf MJ, Murphey MD. Radiologic Evaluation of Soft-Tissue Masses: A Current Perspective. AJR Am J Roentgenol 2000; 175:575-587.
16. Beltran J, Chandnani V, McGhee RA Jr., Kursunoglu-Brahme S. Gadopentetate dimeglumine-enhanced MR imaging of the musculoskeletal system. AJR Am J Roentgenol 1991; 156:457-466.
17. Benedikt RA, Jelinek JS, Kransdorf MJ, Moser RP, Berrey BH. MR imaging of soft-tissue masses: role of gadopentetate dimeglumine. J Magn Reson Imaging 1994; 4:485-490.
18. De Schepper AM, Ramon FA, Degryse HR. Statistical analysis of MRI parameters predicting malignancy in 141 soft tissue masses. Rofo 1992; 156:587-591.
19. Herrlin K, Ling LB, Pettersson H, Willen H, Rydholm A. Gadolinium-DTPA enhancement of soft tissue tumors in magnetic resonance imaging. Acta Radiol 1990; 31:233-236.
20. May DA, Good RB, Smith DK, Parsons TW. MR imaging of musculoskeletal tumors and tumor mimickers with intravenous gadolinium: experience with 242 patients. Skeletal Radiol 1997; 26:2-15.
21. Pettersson H, Eliasson J, Egund N, et al. Gadolinium-DTPA enhancement of soft tissue tumors in magnetic resonance imaging--preliminary clinical experience in five patients. Skeletal Radiol 1988; 17:319-323.

22. Rosenthal RE, Wozney P. Diagnostic value of gadopentetate dimeglumine for 1.5-T MR imaging of musculoskeletal masses: comparison with unenhanced T1- and T2-weighted imaging. J Magn Reson Imaging 1991; 1:547-551.
23. Erlemann R, Reiser MF, Peters PE, et al. Musculoskeletal neoplasms: static and dynamic Gd-DTPA--enhanced MR imaging. Radiology 1989; 171:767-773.
24. Ma LD, Frassica FJ, McCarthy EF, Bluemke DA, Zerhouni EA. Benign and malignant musculoskeletal masses: MR imaging differentiation with rim-to-center differential enhancement ratios. Radiology 1997; 202:739-744.
25. van der Woude HJ, Verstraete KL, Hogendoorn PC, Taminiau AH, Hermans J, Bloem JL. Musculoskeletal tumors: does fast dynamic contrast-enhanced subtraction MR imaging contribute to the characterization? Radiology 1998; 208:821-828.
26. Verstraete KL, De Deene Y, Roels H, Dierick A, Uyttendaele D, Kunnen M. Benign and malignant musculoskeletal lesions: dynamic contrast-enhanced MR imaging--parametric "first-pass" images depict tissue vascularization and perfusion. Radiology 1994; 192:835-843.
27. Verstraete KL, Dierick A, De Deene Y, Uyttendaele D, Vandamme F, Roels H et al. First-pass images of musculoskeletal lesions: a new and useful diagnostic application of dynamic contrast-enhanced MRI. Magn Reson Imaging 1994; 12:687-702.
28. Fletcher BD, Hanna SL. Musculoskeletal neoplasms: dynamic Gd-DTPA-enhanced MR imaging. Radiology 1990; 177:287-288.
29. Beltran J, Simon DC, Katz W, Weis LD. Increased MR signal intensity in skeletal muscle adjacent to malignant tumors: pathologic correlation and clinical relevance. Radiology 1987; 162:251-255.
30. Panicek DM, Go SD, Healey JH, Leung DH, Brennan MF, Lewis JJ. Soft-tissue sarcoma involving bone or neurovascular structures: MR imaging prognostic factors. Radiology 1997; 205:871-875.
31. Verstraete KL, Achten E, Dierick A (1992). Dynamic contrast-enhanced MRI of musculoskeletal neoplasms: different types and slopes of time-intensity curves (abstr). In: Book of abstracts: Society of Magnetic Resonance in Medicine 1992. Berkeley, Calif: Society of Magnetic Resonance in Medicine, pp 2609.
32. Lemeshow S, Hosmer DW Jr. A review of goodness of fit statistics for use in the development of logistic regression models. Am J Epidemiol 1982; 115:92-106.
33. Metz CE. Basic principles of ROC analysis. Semin Nucl Med 1978; 8:283-298.
34. van Erkel AR, Pattynama PM. Receiver operating characteristic (ROC) analysis: basic principles and applications in radiology. Eur J Radiol 1998; 27:88-94.
35. Verstraete KL, Vanzieleghem B, De Deene Y, et al. Static, dynamic and first-pass MR imaging of musculoskeletal lesions using gadodiamide injection. Acta Radiol 1995; 36:27-36.
36. Enzinger FM, Weiss SW. Soft tissue tumors. St. Louis: Mosby, 1995.
37. Heslin MJ, Lewis JJ, Woodruff JM, Brennan MF. Core needle biopsy for diagnosis of extremity soft tissue sarcoma. Ann Surg Oncol 1997; 4:425-431.
38. Barth RJ, Jr., Merino MJ, Solomon D, Yang JC, Baker AR. A prospective study of the value of core needle biopsy and fine needle aspiration in the diagnosis of soft tissue masses. Surgery 1992; 112:536-543.
39. De Schepper AM, De Beuckeleer L, Vandevenne J, Somville J. Magnetic resonance imaging of soft tissue tumors. Eur Radiol 2000; 10:213-223.
40. Shapeero LG, Vanel D, Verstraete KL, Bloem JL. Dynamic Contrast-Enhanced MR Imaging for Soft Tissue Sarcomas. Semin Musculoskelet Radiol 1999; 3:101-114.
41. Ma LD, McCarthy EF, Bluemke DA, Frassica FJ. Differentiation of benign from malignant musculoskeletal lesions using MR imaging: pitfalls in MR evaluation of lesions with a cystic appearance. AJR Am J Roentgenol 1998; 170:1251-1258.
42. van Rijswijk CS, Hogendoorn PC, Taminiau AH, Bloem JL. Synovial sarcoma: dynamic contrast-enhanced MR imaging features. Skeletal Radiol 2001; 30:25-30.